ARTICLES

Laser-Initiated NO Reduction by NH_3: Total Rate Constant and Product Branching Ratio Measurements for the NH_2 + NO Reaction

J. Park and M. C. Lin*

Department of Chemistry, Emory University, Atlanta, Georgia 30322

Received: May 30, 1996; In Final Form: October 9, 1996[⊗]

The total rate constant for the NH_2 + NO reaction has been measured in the temperature range 305−1037 K using a laser photolysis mass spectrometric technique by probing the rates of H_2O formation and NO decay. A weighted least-squares analysis of our data gives the following total rate constant expression: $k_t = 8.29 \times 10^{13}T^{-0.57}$ exp(300/T) cm^3/(mol s). The branching ratios for the two product channels of the NH_2 + NO reaction, N_2H + OH (α) and N_2 + H_2O (β), have also been measured in the temperature range 300−1200 K by detecting CO_2 (formed by the reaction of OH as the added CO) and NO for α and H_2O for β. The value of α was found to increase gradually from 0.1 at 300 K to 0.28 at 1000 K, with a concomitant decrease in β from 0.9 at 300 K to 0.72 at 1000 K. At temperatures between 1000 and 1200 K, α rapidly increases to 0.47 according to the result of our modeling of observed NO decay rates. The drastic upturn in the value of α above 1000 K confirms the results of our recent study of the NH_3 + NO reaction by FTIR spectrometry as well as the conclusion reached by modeling of NH_3−NO flame speeds that α ≥ 0.5 above 1500 K. The absolute rate constants of the two branching reactions are recommended for future applications over the temperature range 300−2000 K.

Introduction

The NH_2 + NO reaction is a key NO removal step in the thermal reduction of NO_x by NH_3[1−4] and by HNCO.[5−10] The reaction is known to occur by both the radical and molecular product routes:[11−20]

$$NH_2 + NO \rightarrow N_2H + OH \quad (1)$$

$$\rightarrow N_2 + H_2O \quad (2)$$

whose branching ratios strongly affect the efficiencies of these reducing agents (i.e., NH_3 and HNCO). This is because reaction 1 effectively produces two key chain carriers, OH and H, on account of the instability of the N_2H radical at high temperatures.

We have demonstrated that the branching ratio for reaction 1, $\alpha = k_1/(k_1 + k_2)$, increases sharply from 0.3 to 0.5 at temperatures between 1000 and 1200 K,[20] bridging the gap between the low-temperature values of α ≤ 0.3 and the recently reported large branching ratios (α ≅ 0.5−0.9) above 1500 K obtained by NH_3−NO flame speed modeling.[21,22] In a brief report which appeared most recently in this journal, we showed by a direct product measurement that in the temperature range 300−1000 K α increases steadily from 0.11 to 0.30 with a concomitant decrease in the value of $\beta = k_2/(k_1 + k_2)$ from 0.89 to 0.70, illustrating for the first time that $\alpha + \beta = 1$.[23]

In this article, we present the results of our new measurements for the total rate constant in the temperature range 305−1037 K and a new set of data for α covering the critical temperature range 1000−1200 K, using a pulsed laser photolysis−mass spectrometric technique. The result of this study independently confirms the drastic increase of α in this critical temperature range which is beneficial to the de-NO_x process.

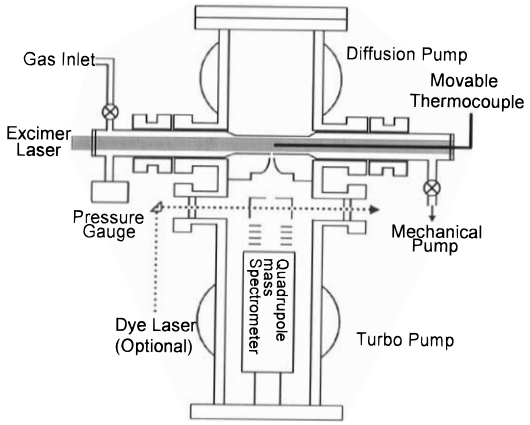

Figure 1. Schematic diagram of the experimental apparatus.

Experimental Section

The total rate constant and branching ratio measurements for the NH_2 + NO reaction were carried out mass spectrometrically using the high-pressure sampling technique developed by Saalfeld and co-workers.[24] The sampling technique has been extensively utilized by Gutman,[25] Matsui, Koshi and their collaborators[26] for kinetic measurements. A schematic diagram of the experimental apparatus is shown in Figure 1. The NH_2

* Corresponding author. E-mail address: chemmcl@emory.edu.
⊗ Abstract published in *Advance ACS Abstracts,* December 1, 1996.

S1089-5639(96)01568-X CCC: $14.00

radical was generated photolytically with an excimer laser (Lambda Physik EMG 102) in a quartz tubular Saalfeld-type reaction tube which has an i.d. of 10 mm and a length of 150 mm with a conical sampling hole of 120 μm diameter at the center of the reactor. The reactor was mounted perpendicularly to the detection axis of a quadrupole mass spectrometer (QMS, Extrel Model C50). For elevated-temperature experiments, the reaction tube was heated with Nichrome ribbon 0.15 mm thick and 15 mm wide and insulated with ceramic wool. By adjusting the current with a variac through the heater, the reaction tube temperature could be varied from 300 to 1200 K. The temperature was measured using a movable type K thermocouple, located near the center of the reaction tube with an accuracy and uniformity of 2 K.

The detection chamber housing the mass spectrometer was separated from the supersonic expansion chamber which holds the reaction tube by a metal plate with a 1.0 mm orifice skimmer (Beam Dynamics Model 1) mounted at the center and 3.0 mm from the sampling hole in the reaction tube. The expansion chamber was pumped by an Edwards Diffstak Model 160/700 diffusion pump with a pumping speed of 1300 L/s to a chamber base pressure of 10^{-7} Torr. The detection chamber was pumped by a Leybold turbomolecular pump with a speed of 1000 L/s to a chamber base pressure of 10^{-8} Torr. The reaction tube was pumped by an Edward rotary vacuum pump with an oil trap to prevent the back-diffusion of oil vapor. During the experiment, the pressures in the expansion and detection chambers were kept at $(5-10) \times 10^{-5}$ and $(5-10) \times 10^{-6}$ Torr, respectively. These conditions produced from the sampling hole a molecular beam which was introduced through the skimmer into the ionization region of the spectrometer.

All experiments were carried out under slow-flow conditions. Mixing of reactants and the helium buffer gas was achieved in a stainless bellows tube prior to the introduction into the reaction tube. The concentration of each individual molecule was obtained by the following formula: $[R] = 9.66 \times 10^{16}(\%)PF_R/TF_T$ molecules/cm^3, where % is the percentage of each molecule in its gas mixture, P is the total reaction pressure in Torr, T is the reaction temperature, F_R is the flow rate of each gas mixture, and F_T is the total flow rate of all gases. The flow rates were measured by using mass flowmeters (Brooks, Model 5850C and MKS, 0258C), and the gas pressure was measured with an MKS Baratron manometer.

NH_3 (Aldrich), CO (Matheson), CO_2 (Aldrich), and H_2O (deionized water) were purified by standard trap-to-trap distillation. NO (Matheson) was purified by vacuum distillation through a silica gel trap maintained at 195 K to remove impurities such as NO_2. The trap was preheated and diffusion pumped for 12 h at 420 K to remove any condensed water. He (99.9995%, Specialty Gases) was used without further purification.

Results

A. Total Rate Constant Measurement. The NH_2 radical was produced by the photolysis of NH_3 at 193 nm at which NH_3 may be photofragmented by the energetically accessible paths

$$NH_3 + h\nu\ (193\ nm) \rightarrow NH_2(X\ ^2B_1) + H(^2S)$$

$$\rightarrow NH_2(A\ ^2A_1) + H(^2S)$$

$$\rightarrow NH(a\ ^1\Delta) + H_2(^1\Sigma_g^+)$$

In the photolysis process, the NH_2 product channel in the electronic ground state is the most dominant ($\Phi = 0.97$). A small amount of NH_2 product ($\Phi = 0.025$) in the electronically excited state could be ignored because of its considerably shorter relaxation time than the title reaction.[26] The NH product is also negligible because of its small quantum yield ($\Phi \leq 0.008$).[26-28] The conversion of NH_3 by photodissociation was 1−8% depending on the reaction temperature and photolysis laser energy (∼30−40 mJ).

The time-resolved concentration of the H_2O product or the NO reactant was directly measured in order to determine the total rate constant for the reaction of NH_2 with NO in the temperature range 305−1037 K using various mixtures of NH_3/NO/He (mainly He diluent). The reaction temperature was limited to 1040 K because of low signal-to-noise ratio caused by high H_2O background or insensitivity of NO signal to the total rate constant because of secondary reactions above that temperature.

Figure 2 shows the time-resolved transient signals of H_2O and NO obtained for kinetic measurements at the selected temperatures. At each, the time-resolved signals were taken for 3−4 different reaction conditions. The positive ion signal was obtained by electron impact ionization at 70 eV followed by QMS mass selection. Transient signals were typically averaged over 200-500 laser shots with a repetition rate of 1 Hz. They were recorded on a Nicolet 450 digital waveform acquisition system. As shown in the inset of the figure, the NH_3 signal dropped immediately after laser firing and remained flat for a period of ∼30 ms until a fresh sample filled the front half of the reaction tube and the NH_3 signal returned to its initial level. During this flat-time period, kinetic and branching ratio measurements were carried out. The repetition rate of 1 Hz allowed enough time between pulses for the NH_3 signal level to return to its initial value.

The experimental conditions for the kinetic measurements were 0.05−0.21 Torr of NH_3 and 0.002−0.062 Torr of NO with $[NO]/[NH_2] = 0.25-50$ and a total pressure of 2.2−9.7 Torr. Under our experimental conditions, we cannot rule out the competing reactions or radical recombination reactions. Thus, time-resolved H_2O and NO concentration profiles were kinetically modeled with the SENKIN program[29] using a set of reactions to simulate the kinetics of the NH_3/NO/He system at each experimental temperature. The solid curves presented in Figure 2 represent the modeled results using the mechanism listed in Table 1 without involving CO.

The results of our total rate constant measurement are summarized in Table 2. A weighted least-squares fit of the rate constants obtained between 305 and 1037 K to the Arrhenius equation yielded

$$k_t = 8.29 \times 10^{13} T^{-0.57} \exp(300/T) \quad \text{cm}^3/(\text{mol s}) \quad (1)$$

B. Branching Ratio Determination. Product channel branching ratios for the NH_2 + NO reaction were measured by the mass-selected detection of H_2O, CO_2, and NO in the temperature range 300−1200 K. The CO_2 product, which resulted from the rapid reaction of OH with added CO, is a convenient and reliable measure of the OH radical present in the system.[30] In order to kinetically model the values of α and β, we kept the total rate constant ($k_t = k_1 + k_2$) of the NH_2 + NO reaction unchanged for each temperature using eq 1, and only the relative values of k_1 and k_2 were varied. The actual number densities of each product were calculated by using its

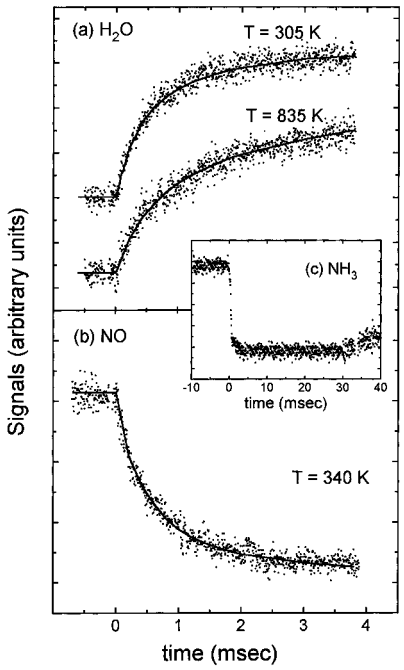

Figure 2. Time-resolved transient signals for the total rate constant measurement of the NH_2 + NO reaction. Conditions are given in Table 2.

signal amplitude at the plateau of the product concentration profile and a carefully prepared calibration gas mixture of H_2O/CO_2/He.[31]

CO_2 and H_2O product measurements for the determination of the branching ratios of the NH_2 + NO reaction were limited to 1000 K because of high H_2O background as mentioned earlier and the possible contamination at m/z 44 caused by N_2O formation from secondary reactions. Thus, NO reactant decay measurement was used for the determination of the branching ratio above 1000 K.

Figure 3 shows the typical transient signals of CO_2 and H_2O products and the NO reactant for branching ratio measurement obtained in the pulsed photolysis of mixtures of NH_3/NO/CO/He and NH_3/NO/He, respectively. The positive ion signals were obtained in the same manner as for kinetic measurement. The slower rise of the signals comparing with those presented in Figure 2 resulted from the use of a higher gain preamplifier in order to get better signal-to-noise ratios in the plateau region.

The typical experimental conditions were 0.05−0.23 Torr of NH_3, 0.00−0.51 Torr of CO, and 0.15−0.34 Torr of NO with $[NO]/[NH_2] = 0.5-1230$ and a total pressure of 2.2−9.7 Torr. In order to account for the radical recombination and other secondary reactions in the calculation of product or reactant number densities, kinetic modeling was carried out with the SENKIN program for each experimental run using the mechanism given in Table 1. Selected experimental conditions for all temperatures studied are summarized in Table 3 with kinetically modeled concentration and branching ratios. The kinetically modeled averaged values of α and β are presented in Figure 4 for comparison with the results reported by several investigators.[2,16,17,19−21]

In addition to the results obtained from the limiting (plateau) concentrations of H_2O for the determination of β, we have acquired more data from kinetic modeling of the time-resolved $[H_2O]_t$ profiles, whose limiting values are controlled by the magnitude of β.

C. Sensitivity Analysis. The key function of the SENKIN program[29] is to compute the value of a sensitivity coefficient (S_{ij}) which reflects the degree of influence by a particular reaction (j) on any species (i) of interest—reactants, products, or reactive intermediates—as a function of reaction time. The sensitivity coefficient is defined by $S_{ij} = (\partial C_i/\partial k_j)(k_j/C_i)$, where C_i is the concentration of the ith species and k_j is the rate constant of the jth reaction included in the mechanism. Effects of key reactions on the removal of NH_2 and NO and the formation of H_2O and CO_2 will be discussed later on the basis of the calculated sensitivity coefficients.

Discussion

A. Total Rate Constant for NH_2 + NO. Many kinetic measurements have been reported for the rate constant of the NH_2 + NO reaction by probing of NH_2 decay[11−16] or OH product formation[17] using a variety of laser-based methods. These results are summarized in Figure 5 as well as in Table 4, which lists the individual rate constants presented in various forms and the experimental methods and conditions employed.

As indicated in the table and the figure, these experimental data have a spread of ±35% from the preferred value taken in the middle of the spread by Baulch et al.[18] In view of the scatter in these data, we attempted to measure the rate constant with the rise time of H_2O production or the decay time of NO using a new, fast amplifier for signal acquisition.

As revealed by the results of sensitivity analyses for NH_2 and H_2O presented in Figure 6, the rates of NH_2 decay and H_2O formation depend strongly on the total rate constant, $k_t = k_1 + k_2$, in the initial stages of the NH_2 + NO reaction. For NH_2, reactions 2 and 13 are responsible for its removal, with large negative sensitivity coefficients. On the other hand, for H_2O, reaction 2 has a positive sensitivity coefficient because it is mainly responsible for its formation. Kinetically, it is understandable why the rise time of H_2O formation depends strongly on k_t, whereas the limiting plateau value of $[H_2O]_t$ is controlled mainly by the branching ratio, $\beta = k_2/k_t$. Accordingly, the absolute values of k_t and β can be simultaneously and independently determined by modeling a single profile of $[H_2O]_t$, such as those shown in Figure 2.

Our kinetically modeled values of k_t are also summarized in Figure 5 and Table 4 for comparison with the published results. As indicated in the figure our results, which can be presented by the expression $k_t = 8.29 \times 10^{13} T^{-0.57} e^{300/T}$ cm^3/(mol s), lie in the middle of the existing scatter and are in close proximity of the preferred values of Baulch et al.[18]

The error limits given in Table 2 for k_t correspond to 1 σ's of the evaluated values which depend predominantly on NH_2 + NO and weakly on secondary reactions. Since our results lie in the middle of the existing scatter (±35%) of k_t's measured by various groups using several techniques throughout the temperature range studied (305−1037 K), they are expected to be reliable within 2 σ's.

B. Product Branching Ratios: α and β. As mentioned in the preceding section, α and/or β have been determined concurrently or independently. For α determination, CO was added to the system and the amount of CO_2 formed by the OH + CO reaction was used to model its value. For β determination, H_2O formed directly in the NH_2 + NO reaction was measured and kinetically modeled for its value. This approach was initially used to determine α and β in the temperature range 300−1060 K.[23]

In the present study, we extended the measurement to cover the critical temperature range in which the value of α was noticed to drastically increase in our recent study of the NH_3 + NO reaction by FTIR spectrometry as indicated above.[20] The rates of the disappearance of NH_3 and NO and that of H_2O

TABLE 1: Reactions and Rate Constants[a] Used in the Modeling of the $NH_2 + NO$ System

	reaction	A	n	E_a	ref
1.	$NH_2 + NO = N_2H + OH$	8.40E+09[e]	0.53	−998	this work[b]
		9.19E+22	−3.02	9589	this work[c]
2.	$NH_2 + NO = N_2 + H_2O$	8.28E+14	−0.93	−382	this work[b]
		3.40E+14	−0.98	−2605	this work[c]
3.	$OH + CO = CO_2 + H$	2.01E+06	1.57	−845	30
4.	$OH + NH_3 = H_2O + NH_2$	2.00E+12	0.00	1830	14
5.	$NH + H = N + H_2$	3.00E+13	0.00	0	4
6.	$NH + N = N_2 + H$	3.00E+13	0.00	0	14
7.	$NH + NH = N_2 + H_2$	2.50E+13	0.00	0	33
8.	$NH + NO = N_2 + OH$	2.90E+13	−0.23	0	4
9.	$NH + NO = N_2O + H$	2.20E+14	−0.40	0	4
10.	$NH + OH = HNO + H$	2.00E+13	0.00	0	4
11.	$NH + OH = N + H_2O$	5.00E+11	0.50	2000	4
12.	$NH + HONO = NH_2 + NO_2$	1.00E+13	0.00	0	35
13.	$NH_2 + H = NH + H_2$	4.00E+13	0.00	3656	33
14.	$NH_2 + HNO = NH_3 + NO$	3.60E+07	1.60	−1252	34
15.	$NH_2 + HONO = NH_3 + NO_2$	7.11E+01	3.00	4942	34
16.	$NH_2 + NH = N_2H_2 + H$	1.50E+15	−0.50	0	33
17.	$NH_2 + NH_2 = NH + NH_3$	5.00E+13	0.00	9995	33
18.	$NH_2 + NH_2 = N_2H_2 + H_2$	5.00E+11	0.00	0	33
19.	$NH_2 + NO_2 = NO + H_2NO$	1.05E+12	0.09	−1156	32
20.	$NH_2 + NO_2 = N_2O + H_2O$	2.47E+11	0.09	−1156	32
21.	$NH_2 + OH + M = H_2NOH + M$	5.70E+24	−3.00	0	14
22.	$NH_2 + OH = NH + H_2O$	4.00E+06	2.00	1000	4
23.	$NH_3 + M = NH_2 + H + M$	2.20E+16	0.00	93468	33
24.	$NH_3 + H = H_2 + NH_2$	6.36E+05	2.39	10171	33
25.	$N_2H + H = H_2 + N_2$	1.00E+14	0.00	0	4
26.	$N_2H + M = H + N_2 + M$	1.00E+14	0.00	3000	14
27.	$N_2H + OH = H_2O + N_2$	5.00E+13	0.00	0	4
28.	$N_2H + NH = NH_2 + N_2$	5.00E+13	0.00	0	33
29.	$N_2H + NO = HNO + N_2$	5.00E+13	0.00	0	4
30.	$N_2H_2 + H = N_2H + H_2$	5.00E+13	0.00	1000	33
31.	$N_2H_2 + O = NH_2 + NO$	1.00E+13	0.00	1000	4
32.	$N_2H_2 + O = N_2H + OH$	2.00E+13	0.00	1000	4
33.	$N_2H_2 + OH = N_2H + H_2O$	1.00E+13	0.00	1000	4
34.	$N_2H_2 + NO = NH_2 + N_2O$	3.00E+12	0.00	0	4
35.	$N_2H_2 + NH = N_2H + NH_2$	1.00E+13	0.00	1000	33
36.	$N_2H_2 + NH_2 = N_2H + NH_3$	1.00E+13	0.00	1000	33
37.	$O + NO_2 = O_2 + NO$	1.00E+13	0.00	600	4
38.	$OH + H_2 = H_2O + H$	1.20E+09	0.00	0	4
39.	$OH + HCO = H_2O + CO$	5.00E+13	0.00	0	36
40.	$OH + HNO = H_2O + NO$	3.60E+13	0.00	0	4
41.	$OH + HONO = H_2O + NO_2$	4.00E+12	0.00	0	35
42.	$OH + NO + M = HONO + M$	1.00E+28	−2.51	−68	35
43.	$OH + OH = H_2O + O$	6.00E+08	1.30	0	4
44.	$OH + OH + M = H_2O_2 + M$	5.70E+24	−3.00	0	14
45.	$H + CH_2O = H_2 + HCO$	2.28E+10	1.10	3279	18
46.	$H + H + M = H_2 + M$	1.00E+18	−1.00	0	4
47.	$H + HCO = H_2 + CO$	9.00E+13	0.00	0	18
48.	$H + HNO = H_2 + NO$	4.50E+11	0.70	650	4
49.	$H + HNCO = NH_2 + CO$	1.10E+14	0.00	12700	36
50.	$H + NO + M = HNO + M$	5.40E+15	0.00	−600	14
51.	$H + NO_2 = OH + NO$	3.50E+14	0.00	1500	4
52.	$H + OH + M = H_2O + M$	1.60E+22	−2.00	0	14
53.	$HCO + HCO = CH_2O + CO$	3.00E+13	0.00	0	18
54.	$HCO + HNO = CH_2O + NO$	2.00E+11	0.70	0	d
55.	$HCO + M = H + CO + M$	1.90E+17	−1.00	17200	36
56.	$HCO + NO = HNO + CO$	7.20E+13	−0.40	0	38
57.	$HNO + O = NO + OH$	1.00E+13	0.00	0	4
58.	$HNO + NO = N_2O + OH$	2.00E+12	0.00	26000	4
59.	$HNO + NO_2 = HONO + NO$	6.00E+11	0.00	2000	35
60.	$HNO + HNO = N_2O + H_2O$	4.00E+12	0.00	5000	4
61.	$HONO + H = NO_2 + H_2$	1.20E+12	0.00	7350	35
62.	$HONO + O = NO_2 + OH$	1.20E+13	0.00	6000	35
63.	$HONO + HONO = NO + NO_2 + H_2O$	2.30E+12	0.00	8400	35
64.	$H_2NO + NO = HNO + HNO$	2.00E+07	2.00	13000	4
65.	$H_2NO + NO_2 = HNO + HONO$	6.00E+11	0.00	2000	35
66.	$H_2NO + NH_2 = HNO + NH_3$	3.00E+12	0.00	1000	35
67.	$HNCO + M = NH + CO + M$	8.41E+15	0.00	84700	36
68.	$HNNO + NO = N_2 + HONO$	2.60E+11	0.00	1620	14
69.	$HNNO + NO = N_2H + NO_2$	3.20E+12	0.00	540	14
70.	$NO_2 + M = NO + O + M$	1.10E+16	0.00	66000	4
71.	$N_2O + M = N_2 + O + M$	4.40E+14	0.00	56100	4

[a] Rate constants are defined by $k = AT^n \exp(-E_a/RT)$ and in units cm^3, mol, and s; E_a is in the unit of cal/mol. [b] For 300−1000 K. [c] For 1000−2000 K. [d] Assumed. [e] Read as 8.40×10^9.

TABLE 2: Summary of the Total Rate Constant Measurements for the NH_2 + NO Reaction[a]

T (K)	P	$[NH_3]_0$	$[NH_2]_0$	$[NO]_0$	k_t (10^{12} cm^3/(mol s))[b]
305	4340−4410	65.65−67.17	5.62−5.75	2.02−4.16	8.59 ± 0.40
305	5090−5190	66.62−67.62	5.93−6.02	3.27−5.51	8.95 ± 0.50
310	2180−9730	62.58−70.87	4.71−5.33	44.34−50.21	8.15 ± 0.50[c]
321	4280−4450	65.99−70.24	5.02−5.16	2.34−7.78	7.91 ± 0.49
340	4360−4700	91.67−92.58	5.41−5.90	1.42−2.50	7.01 ± 0.60
377	5210−5550	67.09−69.22	5.19−5.35	4.05−10.4	6.58 ± 0.45
420	4570−4640	66.28−70.46	5.09−5.41	3.21−7.09	5.59 ± 0.36
473	5460−5960	70.15−74.00	3.24−3.42	4.95−11.1	4.85 ± 0.45
533	4640−4790	68.05−70.47	4.39−4.54	4.38−8.25	4.03 ± 0.48
545	4730−5310	106.4−113.4	1.15−1.18	2.52−4.13	3.80 ± 0.30
660	4720−4930	71.38−75.20	4.08−4.30	5.18−10.8	3.23 ± 0.39
770	5330−6060	131.7−134.9	1.33−1.36	16.7−28.6	3.10 ± 0.35
744	4810−5030	71.32−76.20	3.38−3.61	6.15−12.6	2.87 ± 0.65
835	4910−5250	65.57−74.54	3.21−3.65	8.59−19.7	2.48 ± 0.36
900	4950−6080	73.91−79.09	3.04−3.25	9.09−27.4	2.36 ± 0.25
1037	8000−8510	207.9−211.1	1.25−1.27	31.25−61.5	3.12 ± 0.32

[a] The units of total pressure and all concentrations are in mTorr. [b] Average values from 4−5 experimental runs; the uncertainty represents 1.0σ. [c] Total rate constant was measured with a reactor coated with concentrated H_3PO_4.

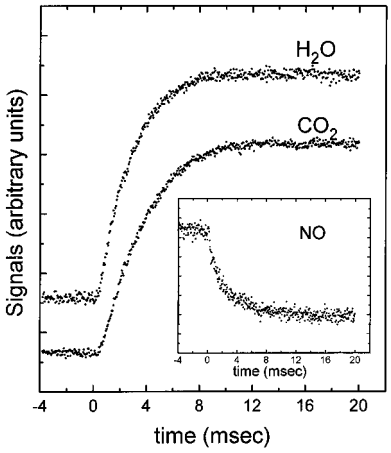

Figure 3. Typical time-resolved transient signals for the branching ratio measurement of the NH_2 + NO reaction.

production determined gravimetrically by Poole and Graven[37] could not be kinetically modeled unless the value of α was raised from 0.30 at 1060 K[23] to 0.5 near 1200 K, the upper limit of the temperature range covered in these pyrolytic studies.

Our present results summarized in Table 3 and Figure 4 quantitatively confirmed the rapid rise of α above 1000 K.[20,23] In addition, the value of β determined below 1060 K also quantitatively demonstrates that $\alpha + \beta = 1$, suggesting that there is no additional product channel present within the temperature range investigated.[23] It was not possible to reliably determine β above 1060 K because of the high H_2O background signal resulting from a significant conversion of the thermal de-NO_x reaction: $4NH_3 + 6NO \rightarrow 5N_2 + 6H_2O$.

In addition to the new values of α determined in the 1000−1200 K region, we have obtained new data for β at nine temperatures from time-resolved H_2O kinetic measurements. These data, denoted by filled circles in the inset of Figure 4, agree closely with the previous results derived from the limiting values of H_2O yields as illustrated in Figure 3 using an amplifier with a higher gain.[23] Figure 7 summarizes the individual branch rate constants, k_1 and k_2, calculated with all values of α, β, and the total rate constant k_t given in eq 1.

Figure 8 shows the results of sensitivity analyses for CO_2 and H_2O products for the system containing NH_3, NO, CO, and He at 800 K. The high sensitivity of the CO_2 yield to the value of k_1 or α is also illustrated in Figure 9, where the yield of CO_2 as a function of time is plotted with varying values of α. At 300 K, a change in α by ±0.05 results in a change of about 50% in $[CO_2]$ plateau yields. Above 1000 K, the same change in α from 0.30 leads to about 16% change in NO conversion, which is readily detectable in our experiments. The results of a sensitivity analysis for NO given in Figure 10 shows that NO decay is strongly affected by reaction 1.

On the basis of our total rate constant for NH_2 + NO and the values of α determined in the present study at 300−1200 K and those reported by Vandooren et al.[21] at 1500−2000 K, the absolute rate constants for reactions 1 and 2 were evaluated by least-squares analysis and are given below (in units of cm^3/(mol s)) for kinetic modeling:

$T = 300-1000$ K

$$k_1 = 8.40 \times 10^9 T^{0.53} e^{+502/T}$$

$$k_2 = 8.28 \times 10^{14} T^{-0.93} e^{+192/T}$$

$T = 1000-2000$ K

$$k_1 = 9.19 \times 10^{22} T^{-3.02} e^{-4826/T}$$

$$k_2 = 3.40 \times 10^{14} T^{-0.98} e^{+1311/T}$$

The branching ratios obtained in the present study over the temperature range 300−1200 K were determined at long reaction times by the limiting concentrations of CO_2, H_2O, and/or NO, which could be reliably measured with standard calibration mixtures. The results of sensitivity analyses for these species indicate that the key secondary reaction affecting their concentrations is the OH + $NH_3 \rightarrow H_2O + NH_2$ reaction, which has been extensively investigated.

To test the effect of the OH + NH_3 reaction on α, we varied its rate constant by ±100% near 1000 K. This led to a concomitant change in the value of $\alpha = 0.28$ by ±0.05 based on CO_2 and by ∓0.03 based on the NO concentration measured. The changes are expected to be smaller below 1000 K and larger near 1200 K. In view of the critical importance of the N_2H + OH branching ratio above 1200 K to the de-NO_x process, a careful shock tube study by OH diagnostics is recommended for the 1000−2000 K range.

C. NO Reduction. The magnitude of α strongly affects the efficiency of NO reduction by NH_3 because the two most reactive chain carriers, H and OH, are produced concurrently by reaction 1. This effect is illustrated by the sensitivity analysis result presented in Figure 10, indicating that the major NO reducing reactions are (1) and (24), H + NH_3, which generates

TABLE 3: Typical Reaction Conditions[a] and Product Yields[b] at Temperature Studied

						$[CO_2]_t$			$[H_2O]_t$			$[NO]_t$			
T (K)	P	$[NH_3]_0$	$[NH_2]_0$	$[CO]_0$	$[NO]_0$	exp	α	calc	exp	β	calc	exp	α	calc	note
300	7200	71.93	2.92	93.64	346.0	0.115	0.10	0.113	2.904	0.90	2.894				*c*
302	6200	59.74	3.01	78.51	264.2	0.119	0.10	0.116	3.003	0.90	3.007				*c*
305	5190	66.62	5.93	0.0	5.5				4.370	0.90	4.391				*d*
310	2180	62.58	4.71	0.0	44.34				4.800	0.90	4.796				*e*
321	4450	65.99	4.85	0.0	7.8				4.280	0.90	4.263				*d*
377	5550	67.09	5.19	0.0	10.4				4.722	0.90	4.551				*d*
420	4600	70.46	5.41	0.0	3.2				3.585	0.88	3.591				*d*
473	5670	70.15	3.24	0.0	11.1				2.721	0.88	2.869				*d*
527	6720	69.38	2.52	89.94	263.9	0.106	0.14	0.104	2.635	0.86	2.628				*d*
533	4790	68.05	4.39	0.0	8.3				2.783	0.84	2.793				*d*
695	6950	57.29	1.11	73.05	293.9	0.048	0.18	0.046	1.088	0.82	1.050				*c*
744	5030	71.32	3.38	0.0	12.6				1.121	0.80	1.127				*d*
800	3900	82.01	2.30	205.7	169.1	0.201	0.20	0.196	2.351	0.80	2.321				*c*
835	5250	65.57	3.21	0.0	19.7				2.167	0.78	2.179				*d*
882	7060	68.26	0.90	86.51	315.3	0.073	0.24	0.076	1.331	0.76	1.370				*c*
900	6080	73.91	3.04	0.0	27.4				2.545	0.78	2.548				*d*
930	4010	86.99	1.24	215.2	172.4	0.194	0.26	0.207	1.988	0.74	2.000				*c*
957	8020	179.5	0.23	513.6	282.4				0.563	0.72	0.532				*d*
1004	4500	100.0	1.22	247.1	188.8	0.279	0.28	0.287	2.467	0.72	2.570				*c*
1016	8100	96.05	0.87	121.3	339.8	0.115	0.26	0.111	2.002	0.74	2.106				*c*
1037	8000	211.1	1.27	0.0	31.25							27.42	0.28	27.36	*f*
1060	4120	89.89	0.91	221.5	179.5	0.256	0.30	0.258	2.203	0.68	2.274				*c*
1095	9500	231.4	2.10	0.0	68.70							62.10	0.36	61.75	*f*
1123	5130	97.61	0.99	0.0	48.89							47.20	0.40	47.15	*f*
1155	4730	109.9	1.00	0.0	43.23							41.35	0.44	41.39	*f*
1170	4730	144.2	1.16	0.0	56.68							54.35	0.46	54.40	*f*
1200	4830	147.6	0.89	0.0	57.88							55.57	0.48	56.03	*f*

[a] The units of total pressure and all concentrations are in mTorr. [b] exp and cal represent the experimental and kinetically modeled concentrations, respectively. [c] The signal amplitude was taken at $t = 15$ ms for CO_2 and $t = 10$ ms for H_2O in their concentration plateau regions. [d] The signal amplitude was taken at $t = 3.5$ ms. [e] The signal amplitude was taken using a reactor coated with concentrated H_3PO_4 at $t = 3.5$ ms. [f] The signal amplitude was taken at $t = 15$ ms.

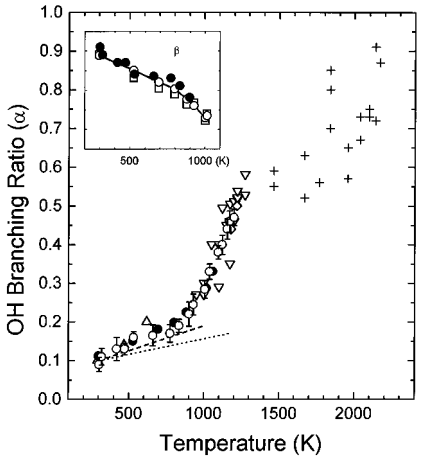

Figure 4. Summary of branching ratios for $NH_2 + NO \rightarrow N_2H + OH$ (α) and $N_2 + H_2O$ (β) as functions of temperature. The results of various studies: dotted line, ref 19; dashed line, ref 17; △, ref 16; ▽, ref 20; ◇, ref 2; +, ref 21; ●, ref 23; ○, this work (α). Inset: ●, this work; ○, ref 23 (β); □, ref 23 (1 − α). The ordinate of the inset is in the same scale of Figure 4.

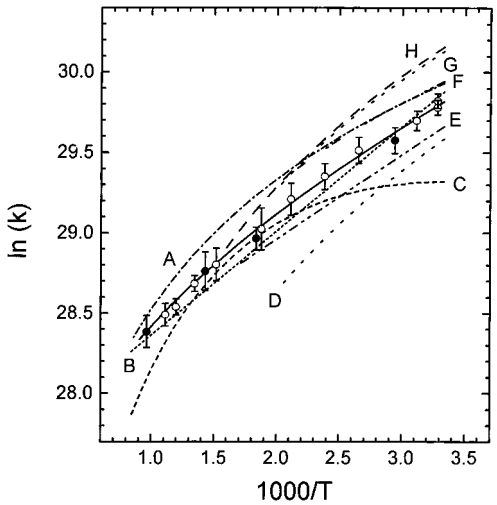

Figure 5. Arrhenius plot for the total rate constant of the $NH_2 + NO$ reaction: A, ref 17; B, ref 18; C, ref 11; D, ref 13; E, ref 14; F, ref 15; G, ref 12; H, ref 16. This work: ○, measured by H_2O; ●, measured by NO; solid curve, fitted results.

more NH_2. The destruction of NH_2, on the other hand, is dominated by the removal processes 2 and 13.

The drastic increase of α from 0.3 at 1000 K to 0.9 at 2000 K according to the NH_3−NO flame speed measurement of Vandooren et al.[21] strongly indicates the efficacy of NH_3 as an NO_x reducing agent.

D. Comments on the Effects of Pressure, Reactant Ratio, and Reactor Surface. In the present experiment, the total pressure was varied from 2 to 10 Torr, limited by the operational range of pressure in the quadrupole mass spectrometer ($P < 10^{-5}$ Torr). The values of k_t, α, and β were affected neither by the total pressure nor by the [NO]/[NH_2] reactant ratio, which was varied over a range of 0.25−1230.

The absence of pressure effect within atmospheric pressure is clearly illustrated by the close agreement among k_t's measured over the wide range of pressure employed in various studies as summarized in Table 4 (1 Torr ≤ P ≤ 700 Torr). Our RRKM calculations carried out earlier[14] on the effects of temperature and pressure on the total rate constant and products branching ratios did not reveal significant dependence of these quantities on pressure either.

To test the possible effect of reactor surface, we have performed an additional measurement with a reactor coated with

TABLE 4: Comparison of Experimental Rate Constant Expression for the NH_2 + NO Reaction

rate constant expression[a]	T (K)	P (Torr)	$10^{-13}k_{300}$[b]	method[c]	ref
$2.64 \times 10^{19}T^{-2.3}\exp(-684/T)$	294−1215	1.0−2.8	0.54	DF/LIF (NH_2)	11
$1.67 \times 10^{17}T^{-1.67}$	216−480	2.5−20	1.22	FP/LIF (NH_2)	12
$2.7 \times 10^{17}T^{-1.85}$	209−505	0.4−4.0	0.71	DF/LIF (NH_2)	13
$1.33 \times 10^{12}\exp(525/T)$	297−673	20−150	0.77	LP/CRD (NH_2)	14
$1.28 \times 10^{16}T^{-1.25}$	300−500	2−700	1.03	FP/AS (NH_2)	15
$3.37 \times 10^{18}T^{-2.2}$	295−620	1−31	1.20	FP/ILS (NH_2)	16
$7.9 \times 10^{15}T^{-1.17}$	294−1027	3−100	1.00	LP/LIF (OH)	17
$1.08 \times 10^{12}\exp(650/T)$	220−2000		0.94	recommended	18
$8.29 \times 10^{13}T^{-0.57}\exp(300/T)$	305−1037	2.2−9.7	0.89	LP/MS (H_2O, NO)	this work

[a] Rate constants are in the units of $cm^3/(mol\ s)$. [b] Rate constant at 300 K. [c] In parentheses, the species probed or measured are indicated. FP = flash photolysis, AS = absorption spectroscopy, DF = dischage flow, LP = laser photolysis, LIF = laser-induced fluorescence, ILS = intracavity laser spectroscopy, CRD = cavity ring down, and MS = mass spectrometry.

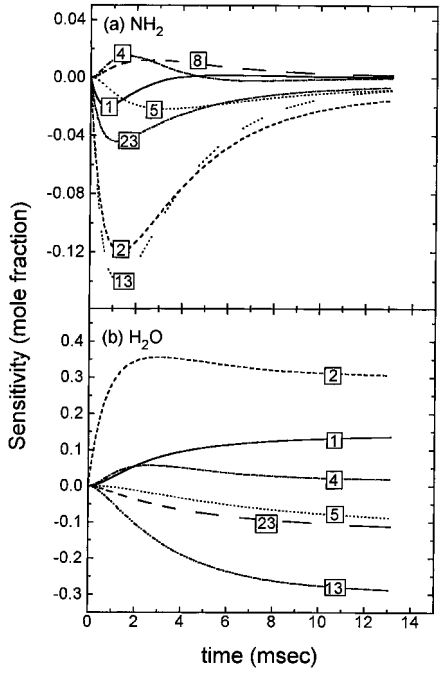

Figure 6. Sensitivity analyses for NH_2 and H_2O formed in the NH_3/NO/He system at 744 K. Conditions are given in Table 3. The method of sensitivity analysis can be found in ref 29.

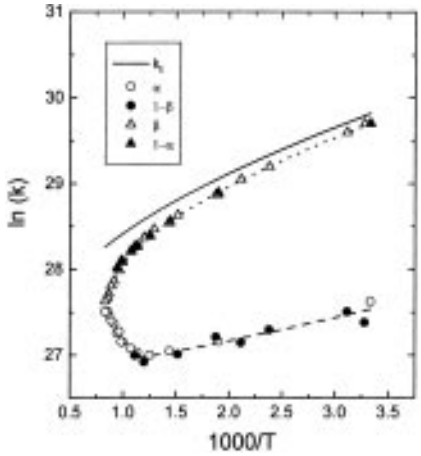

Figure 7. Absolute rate constants for $NH_2 + NO \rightarrow N_2H + OH$ (k_1) and $NH_2 + NO \rightarrow N_2 + H_2O$ (k_2). Open symbols indicate the results of direct measurements.

concentrated H_3PO_4. At the lowest pressure employed in the present study, $P = 2.18$ Torr, the values of both k_t and β measured at 310 K with the coated reactor agree quantitatively with those obtained with uncoated quartz reactors of varying expansion orifices (see Tables 2 for k_t and Table 3 for β).

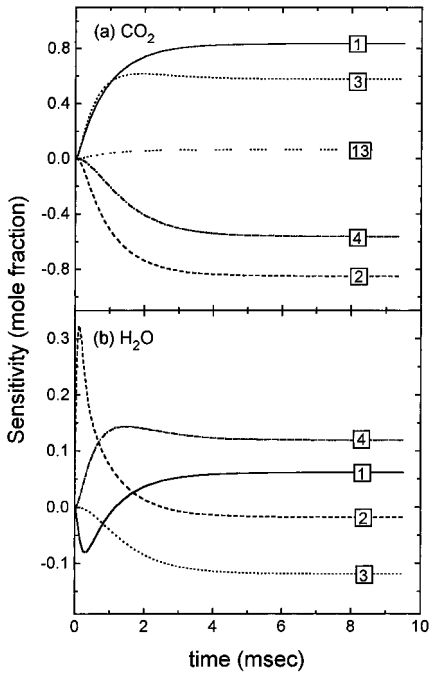

Figure 8. Sensitivity analyses for CO_2 and H_2O formed in the NH_3/NO/CO/He system at 800 K. Conditions are given in Table 3.

The insignificance of reactor surface effects on the values of k_t can also be ascertained by the existence of the close agreement among k_t's measured by a variety of techniques under a wide range of pressure as alluded to above. The remarkable accord in values of α between 950 and 1200 K (see Figure 5) determined by the present laser photolysis/mass spectrometric study at 2−10 Torr pressure and by the kinetic modeling of the data from pyrolytic studies of the NH_3 + NO reaction by FTIR spectrometry at 700 Torr pressure with a static reactor[20] as well as the gravimetric measurement of the H_2O formed at 800 Torr pressure with two different quartz flow tubes[37] also rules out any significant influence of reactor surfaces.

Conclusion

The reaction initiated by pulsed photolysis NH_3−NO mixtures at 193 nm using a high-pressure sampling mass spectrometric technique developed by Saalfeld and co-workers[24] allows us to study the kinetics of NH_2 + NO in detail. From the time-resolved concentration profiles of H_2O and NO measured between 305 and 1037 K, we obtained the total rate constant for NH_2 + NO: $k_t = 8.3 \times 10^{13}T^{-0.57}e^{300/T}\ cm^3/(mol\ s)$, which is in excellent agreement with the preferred literature value.[18]

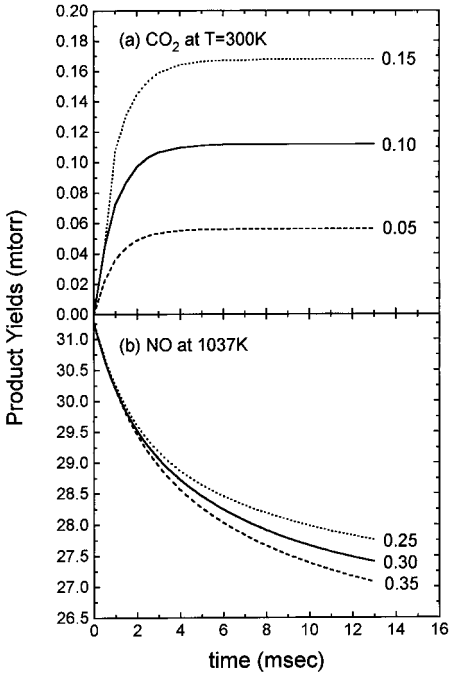

Figure 9. Sensitivity of CO_2 formation and NO decay to the value of α (or k_1). Conditions are given in Table 3.

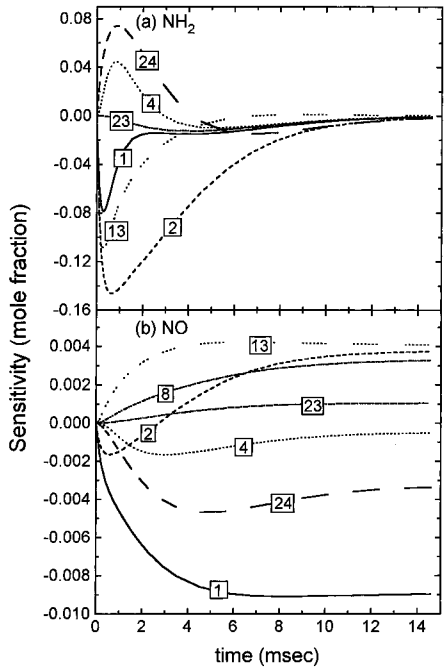

Figure 10. Sensitivity analyses for NH_2 and NO reflecting the efficiency of NO reduction by NH_3 at 1200 K. Conditions are given in Table 3.

From the accurate measurements of absolute yields of H_2O and CO_2, formed by the reaction of OH with added CO, the product channel branching ratios for $NH_2 + NO \rightarrow N_2 + H_2O$ (β) and $NH_2 + NO \rightarrow N_2H + OH$ (α), respectively, have been obtained in the temperature range 300−1060 K. The value of β was found to decrease from 0.90 at 300 K to 0.70 at 1060 K with a concomitant increase in α from 0.10 to 0.30. By kinetic modeling of the NO decay profiles measured between 1000 and 1200 K, we have confirmed the results of our recent pyrolytic study of the $NH_3 + NO$ reaction by FTIR spectrometry[20] that the value of α increases rapidly from 0.3 near 1000 K to 0.47 at 1200 K. The drastic upturn in the value of α supports the conclusion reached recently from kinetic modeling of NH_3−NO flame speeds by Vandooren et al.[21] and by Brown and Smith[22] that $\alpha \geq 0.5$ above 1500 K. These new results strongly suggest that NH_3 is indeed a highly efficient de-NO_x agent.

Theoretically, the rapid increase in α above 1000 K is not clearly understood. The result of a recent variational RRKM calculation by Diau and Smith[39] for the production of $N_2H + OH$ did not reveal any sigmoidal increase in α, although its large value above 1200 K ($\alpha > 0.5$) could be accounted for theoretically. Intuitively, one would expect that the sharp upturn in the value of α above 1000 K might reflect the opening of the new direct, three-body fragmentation process, $HNNOH \rightarrow H + N_2 + OH$ at higher energies. This direct channel should be included in theoretical modeling also.

Acknowledgment. The authors gratefully acknowledge the support of this work by the Office of Naval Research (Contract N00014-89-J-1949) under the direction of Dr. R. S. Miller. We thank the Cherry L. Emerson Center for Scientific Computation for the use of computing facilities and various programs.

Note Added in Proof: In Table 4 and Figure 5, we inadvertently left out the recent result of M. Wolf, D. L. Yang, and J. L. Durant which appeared in *J. Photochem. Photobiol.* **1994**, *A80*, 85, for the total rate constant of the $NH_2 + NO$ reaction, $k_t = 3.3 \times 10^{24} T^{-4.02} e^{-1034/T}$ cm^3/(mol s). This is in close agreement with the majority of the published data summarized.

References and Notes

(1) Miller, J. A.; Branch, M. C.; Kee, R. J. *Combust. Flame* **1981**, *43*, 81.
(2) Kimball-Linne, M. A.; Hanson, R. K. *Combust. Flame* **1986**, *64*, 377.
(3) Lyon, R. K. *Int. J. Chem. Kinet.* **1976**, *8*, 318; U.S. Patent 3,900,554.
(4) Glarborg, P.; Dam-Johansen, K.; Miller, J. A.; Kee, R. J.; Coltrin, M. E. *Int. J. Chem. Kinet.* **1994**, *26*, 421.
(5) Perry, R. A.; Siebers, D. L. *Nature* **1986**, *324*, 657.
(6) Wicke, B. G.; Grady, K. A.; Ratcliffe, J. W. *Combust. Flame* **1989**, *78*, 249.
(7) Caton, J. A.; Siebers, D. L. *Combust. Sci. Technol*. **1989**, *65*, 277.
(8) Lyon, R. K.; Cole, J. A. *Combust. Flame* **1990**, *82*, 435.
(9) Miller, J. A.; Bowman, C. T. *Int. J. Chem. Kinet.* **1991**, *23*, 289.
(10) Mertens, J. D.; Chang, A. Y.; Hanson, R. K.; Bowman, C. T. *Int. J. Chem. Kinet.* **1991**, *23*,173.
(11) Silver, J. A.; Kolb, C. E. *J. Phys. Chem.* **1982**, *86*, 3240.
(12) Stief, L. J.; Brobst, W. D.; Nava, D. F.; Borkowski, R. P.; Michael, J. V. *J. Chem. Soc., Faraday Trans. 2* **1982**, *78*, 1391.
(13) Hack, W.; Schake, H.; Schröter, H.; Wagner, H. Gg. *17th Symposium (International) on Combustion;* The Combustion Institute: Pittsburgh, PA, 1979; p 505.
(14) Diau, E. W. G.; Yu, T.; Wagner, M. A. G.; Lin, M. C. *J. Phys. Chem.* **1994**, *98*, 4034.
(15) Lesclaux, R.; Khê, Pham Van; Dezauzier, P.; Soulignac, J. C. *Chem. Phys. Lett.* **1975**, *35*, 493.
(16) Bulatov, V. P.; Ioffe, A. A.; Lozovsky, V. A.; Sarkisov, O. M. *Chem. Phys. Lett.* **1989**, *161*, 141.
(17) Atakan, B.; Jacobs, A.; Wahl, M.; Weller, R.; Wolfrum, J. *Chem. Phys. Lett.* **1989**, *155*, 609.
(18) Baulch, D. L.; Cobos, C. J.; Cox, R. A.; Esser, C.; Frank, P.; Just, Th.; Kerr, J. A.; Pilling, M. J.; Troe, J.; Walker, R. W.; Warnatz, J. J. *Phys. Chem. Ref. Data* **1992**, *21*, 411.
(19) Stephens, J. W.; Morter, C. L.; Farhat, S. K.; Glass, G. P.; Curl, R. F. *J. Phys. Chem.* **1993**, *97*, 8944.
(20) Halbgewachs, M. J.; Diau, E. W. G.; Mebel, A. M.; Lin, M. C.; Melius, C. F. *26th Symposium (International) on Combustion*, in press.
(21) Vandooren, J.; Bian, J.; van Tiggelen, P. J. *Combust. Flame* **1994**, *402*.
(22) Brown, M. J.; Smith, D. B. *25th Symposium (International) on Combustion*; The Combustion Institute: Pittsburgh, PA, 1994; p 1011.
(23) Park, J.; Lin, M. C. *J. Phys. Chem.* **1996**, *100*, 3317.

(24) Wyatt, J. R.; DeCorpo, J. J.; McDowell, M. V.; Saalfeld, F. E. *Rev. Sci. Instrum.* **1974**, *45*, 916; *Int. J. Mass Spectrom. Ion Phys*. **1975**, *16*, 33.
(25) Slagle, I. R.; Gutman, D. *J. Am. Chem. Soc.* **1985**, *107*, 5342. Russell, J. J.; Seetula, J. A.; Gutman, D. *Ibid.* **1988**, *110*, 3092.
(26) Koshi, M.; Miyoshi, A.; Matsui, H. *J. Phys. Chem.* **1991**, *95*, 9869
(27) Donelly, V. M.; Baronavski, A. P.; McDonald, J. R. *Chem. Phys.* **1979**, *43*, 271, 283.
(28) Halpern, J. B.; Hancock, G.; Lenzi, M.; Welge, K. H. *J. Chem. Phys.* **1975**, *63*, 4808.
(29) Lutz, A. E.; Kee, R. J.; Miller, J. A. SENKIN: A FORTRAN Program for Predicting Homogeneous Gas-Phase Chemical Kinetics with Sensitivity Analysis; Sandia National Laboratories, Report SAND87-8248, 1988.
(30) Ravishankara, A. R.; Thompson, R. L. *Chem. Phys. Lett.* **1983**, *99*, 377.
(31) Four different H_2O, CO_2, and He mixtures were used to calibrate the *m*/*z* 18 and 44 signals for individual runs. The Pyrex bulbs employed for these calibration mixtures were first saturated with several Torr of H_2O and then evacuated for preparation of samples. The H_2O concentrations obtained from the *m*/*z* 18 signals using various calibration mixtures agreed closely.
(32) Park, J.; Lin, M. C. Mass-Spectrometric Determination of Product Branching Probabilities for the $NH_2 + NO_2$ Reaction at Temperatures between 300 and 990 K. *Int. J. Chem. Kinet.*, in press.
(33) Davidson, D. F.; Koshe-Hoinghaus, K.; Chang, A. Y.; Hanson, R. K. *Int. J. Chem. Kinet.* **1990**, *22*, 513.
(34) Mebel, A. M.; Diau, E. W. G.; Lin, M. C.; Morokuma, K. *J. Phys. Chem.*, in press.
(35) Glarborg, P.; Dam-Johansen, K.; Miller, J. A. *Int. J. Chem. Kinet.* **1983,** *27*, 1207.
(36) Wu, C. H.; Wang, H.-t., Lin, M. C.; Fifer, R. A. *J. Phys. Chem*. **1990**, *94*, 3344.
(37) Poole, D. R.; Graven, W. M. *J. Am. Chem. Soc*. **1961**, *83*, 283.
(38) Veyret, B.; Lesclaux, R. *J. Phys. Chem.* **1981**, *85*, 1918.
(39) Diau, E. W. G.; Smith, S. C. Private communication.